

# **Advanced Underwater Imaging Phase IV Annual Report FY08**

PI: Fraser R. Dagleish

Harbor Branch Oceanographic Institute

5600 US Hwy 1 North, Fort Pierce, FL 34946

phone: (772) 360-9991 fax: (772) 464-9094 email: [fdalglei@hboi.fau.edu](mailto:fdalglei@hboi.fau.edu)

co-PI: Frank M. Caimi

Harbor Branch Oceanographic Institute

5600 US Hwy 1 North, Fort Pierce, FL 34946

phone: (772) 713-1147 fax: (772) 464-9094 email: [frankstir@gmail.com](mailto:frankstir@gmail.com)

Grant Number: N000140610113

## **LONG-TERM GOALS**

The overall objective of the Advanced Underwater Imaging (AUI) program is to advance the state-of-the-art in wide-swath underwater laser imaging with the long-term goal of transitioning this technology to the Navy's fleet of 21" diameter and smaller form factor autonomous underwater vehicles (AUVs).

## **OBJECTIVES**

Following the development and refinement of benchtop pulsed laser line scan (PLLS) imaging hardware and image simulation tools in FY07, the objectives of the work performed during this funding period were to:

1. Perform experimental validation of time history code for underwater PLLS model
2. Experimental comparison of CW/pulsed/ modulated-pulse variants of LLS
3. Analytic comparison between CW/pulsed/modulated-pulse variants of LLS
4. Application of image quality algorithms to acquired images
5. Complete experimental hardware to allow for wide-swath LLS imaging

## **APPROACH**

The approach for meeting these objectives within this funding period involved continuing collaborations with Physical Sciences Inc (Andover, MA) and Metron Inc (Reston, VA) in the areas of image analysis and radiative transfer modeling. In summary the proposed technical approach consisted of the following activities:

1. Rigorous test tank validation of laser pulse time history model, including experimental measurement of beam spread function over extended distances.
2. Development of a receiver model as a necessary addition to the EODES-3 software to more accurately simulate the major noise sources present in the image formation process for both pulsed and CW LLS.
3. Test tank comparison between CW LLS and gated-PLLS imagers.
4. Application of Image Quality algorithms to acquired images.

<b>Report Documentation Page</b>			Form Approved OMB No. 0704-0188					
<p>Public reporting burden for the collection of information is estimated to average 1 hour per response, including the time for reviewing instructions, searching existing data sources, gathering and maintaining the data needed, and completing and reviewing the collection of information. Send comments regarding this burden estimate or any other aspect of this collection of information, including suggestions for reducing this burden, to Washington Headquarters Services, Directorate for Information Operations and Reports, 1215 Jefferson Davis Highway, Suite 1204, Arlington VA 22202-4302. Respondents should be aware that notwithstanding any other provision of law, no person shall be subject to a penalty for failing to comply with a collection of information if it does not display a currently valid OMB control number.</p>								
1. REPORT DATE <b>2008</b>	2. REPORT TYPE	3. DATES COVERED <b>00-00-2008 to 00-00-2008</b>						
<b>4. TITLE AND SUBTITLE</b> <b>Advanced Underwater Imaging Phase IV Annual Report FY08</b>			5a. CONTRACT NUMBER					
			5b. GRANT NUMBER					
			5c. PROGRAM ELEMENT NUMBER					
<b>6. AUTHOR(S)</b>			5d. PROJECT NUMBER					
			5e. TASK NUMBER					
			5f. WORK UNIT NUMBER					
<b>7. PERFORMING ORGANIZATION NAME(S) AND ADDRESS(ES)</b> <b>Harbor Branch Oceanographic Institute, 5600 US Hwy 1 North, Fort Pierce, FL, 34946</b>			8. PERFORMING ORGANIZATION REPORT NUMBER					
<b>9. SPONSORING/MONITORING AGENCY NAME(S) AND ADDRESS(ES)</b>			10. SPONSOR/MONITOR'S ACRONYM(S)					
			11. SPONSOR/MONITOR'S REPORT NUMBER(S)					
<b>12. DISTRIBUTION/AVAILABILITY STATEMENT</b> <b>Approved for public release; distribution unlimited</b>								
13. SUPPLEMENTARY NOTES								
14. ABSTRACT								
15. SUBJECT TERMS								
<b>16. SECURITY CLASSIFICATION OF:</b>  <table border="1"> <tr> <td>a. REPORT <b>unclassified</b></td> <td>b. ABSTRACT <b>unclassified</b></td> <td>c. THIS PAGE <b>unclassified</b></td> </tr> </table>			a. REPORT <b>unclassified</b>	b. ABSTRACT <b>unclassified</b>	c. THIS PAGE <b>unclassified</b>	<b>17. LIMITATION OF ABSTRACT</b> <b>Same as Report (SAR)</b>	<b>18. NUMBER OF PAGES</b> <b>9</b>	<b>19a. NAME OF RESPONSIBLE PERSON</b>
a. REPORT <b>unclassified</b>	b. ABSTRACT <b>unclassified</b>	c. THIS PAGE <b>unclassified</b>						

5. Comparison of EODES-3 image simulation results with real PLLS images.
6. More advanced simulations and experimental validation for alternate laser sources, such as modulated-pulsed lasers.
7. Use the validated models and known hardware constraints to explore the design issues, limitations and associated performance implications for CW, pulsed, and modulated-pulse line scanning system alternatives.

## WORK COMPLETED

### 1. Experimental validation of laser pulse time history code

A series of experiments was conducted with a pulsed laser in the HBOI imaging test facility to validate the performance of the computational model. Scattering was varied by the addition of Maalox and optical properties were measured with a WET Labs ac-9 meter. Parameters such as receiver aperture, source-receiver separation, the pointing angle of the receiver and the turbidity of the water were systematically varied and a series of pulse time histories were recorded at a 5 GHz sampling rate for each set of conditions. The measured and modeled results were then compared. Discrepancies were evaluated to determine if the issue lay with the model or with the experiment.

### 2. Test-tank imager comparison between gated-PLLS and CW LLS

A series of experiments was conducted in the imaging test facility at realistic stand-off distances in a variety of turbidity conditions ranging from very clear conditions to greater than 7 attenuation lengths. Scattering was varied by the addition of Maalox and optical properties were measured with the ac-9 meter. System parameters were adjusted to allow for a fair comparison (equal energy per pixel). The USAF-1951 white-on-black target was mainly used for this study. It was chosen due to the ease of qualitatively observing the reduction in backscatter and shot noise possible with the pulsed-gated imagers.

### 3. Application of Image Quality algorithms to acquired images.

The acquired images were analyzed using a variety of image quality metrics to compare the relative contrast and signal-noise ratios versus attenuation coefficient and stand-off distance. Image quality metrics for two applications of image analysis were investigated: optimizing image quality in the field during image acquisition by an autonomous system, and comparing images of test targets obtained in the HBOI imaging facility. In the field the challenge is ensuring that an imaging system is acquiring the best possible images under the operating conditions that exist at the time, which might require adjusting system configuration parameters, while in the laboratory the need is to evaluate the impacts of controlled changes in experimental parameters, or to compare the performance of alternative imaging configurations. For the field application, approaches were investigated that are used for autofocus in digital cameras. These systems vary the lens position, compute a sharpness metric from the image at each position, and then set the lens at the best position according to the metric. The analogy for a laser imaging system in the field, is that parameters such as alignment angle could be varied, and the images compared in a similar manner. Based on the results reported in Shih (2007), which compared a wide variety of autofocus metrics in a systematic way, we selected the Tenengrad-Sobel (T-S) metric for further experimentation. The Tenengrad/Sobel algorithm adopts a 2D spatial gradient measurement approach for sharpness determination. A typical operator uses a 3x3 or larger matrix to detect edges in the horizontal and vertical directions. For each image pixel, the algorithm

derives two fitness values based on the horizontal and vertical neighbors, and these are then used collectively to determine the overall fitness value. Intuitively, these fitness values represent the gradient magnitudes at each point in the image.

$$\begin{array}{ccc}
 & -1 & 0 & 1 \\
 \mathbf{G}_x & -2 & 0 & 2 \\
 & -1 & 0 & 1
 \end{array}
 \quad
 \begin{array}{ccc}
 & 1 & 2 & 1 \\
 \mathbf{G}_y & 0 & 0 & 0 \\
 & -1 & -2 & -1
 \end{array}$$

The overall fitness function is then given (for an M x N matrix) by:

$$F(i, j) = \sum_{i=1}^M \sum_{j=1}^N \sqrt{G_x(i, j)^2 + G_y(i, j)^2}$$

For laboratory work we applied the T-S algorithm, but in addition applied several contrast and signal to noise algorithms for the technical target work, specifically a conventional contrast ratio and the contrast signal noise ratio:

$$\text{Contrast ratio: } \frac{\text{WhiteMean} - \text{BlackMean}}{\text{WhiteMean} + \text{BlackMean}}$$

$$\text{Contrast SN ratio: } \frac{\text{WhiteMean} - \text{BlackMean}}{\sqrt{\text{WhiteSTD}^2 + \text{BlackSTD}^2}}$$

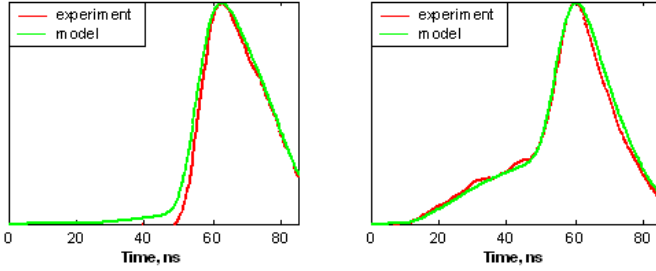
The contrast ratios were computed for raw target images with means and standard deviations computed over adjacent ‘black’ and ‘white’ areas of the technical target, as well as for images after application of processes such as normalization, median filtering, and histogram equalization. The computed values help in comparing images both between and within system types.

#### 4. Advanced simulations and experimental validation for modulated-pulses.

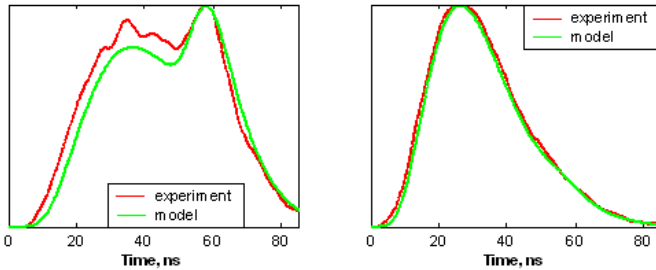
Utilizing the latest Metron code with finer time resolution, it had been possible in the FY07 funding period to investigate the benefits of several alternative modulated-pulse coding schemes. These techniques show potential to make improvement in achievable signal-to-noise ratio and timing resolution by careful selection of modulation code and suitable coherent processing algorithm. To produce experimental results supporting this study, a 500ps (40μJ per pulse) green laser was used with a series of beam splitters and mirrors with appropriate delay times to generate a 1GHz amplitude modulation tone. Experiments were conducted through greater than 11 meters of turbid water to compare with simulations results. An additional processing stage was implemented to investigate the enhanced detection of the modulated-pulse using IQ demodulation techniques.

## RESULTS

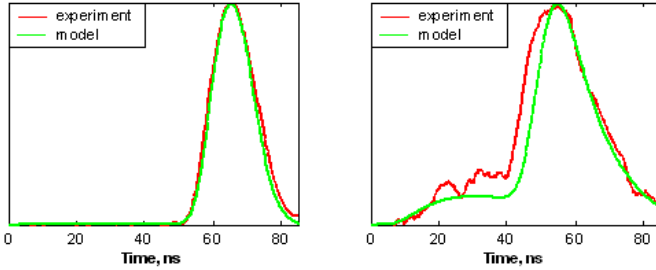
### 1. Validation comparisons of laser pulse time history code



*Graphs of the experimental data (red) and model results (green). Left:  $c=0.08 \text{ m}^{-1}$ , SR=376mm, aperture = 3mm. Right:  $c=0.25 \text{ m}^{-1}$ , SR=376mm, aperture = 3mm.*



*Graphs of the experimental data (red) and model results (green). Left:  $c=0.48 \text{ m}^{-1}$ , SR=376mm, aperture = 3mm. Right:  $c=0.63 \text{ m}^{-1}$ , SR=376mm, aperture = 3mm.*



*Graphs of the experimental data (red) and model results (green). Left:  $c=0.06 \text{ m}^{-1}$ , SR=250mm, aperture = 1mm. Right:  $c=0.25 \text{ m}^{-1}$ , SR=83mm, aperture = 1mm.*

**Figure 1: Some results from the experimental validation of the Metron underwater laser pulse time history simulation software.**

The model has proven to be a good predictor of pulse behavior, and the validation effort supports its use as a design tool for the development of the gated-PLLS imaging system.

### 2. Test tank imager comparison between gated-PLLS and CW LLS.

It can be seen from fig. 2 that as the number of attenuation lengths approaches the limiting scenario, there is significantly less noise present in the simulated images, particularly for the CW LLS case. Due to this consistent discrepancy, it appeared necessary to also simulate the noise generated in both types

of receiver to increase the fidelity of the image performance prediction code. The next version of the Metron EODES-3 code (released October 2008) will have that capability.

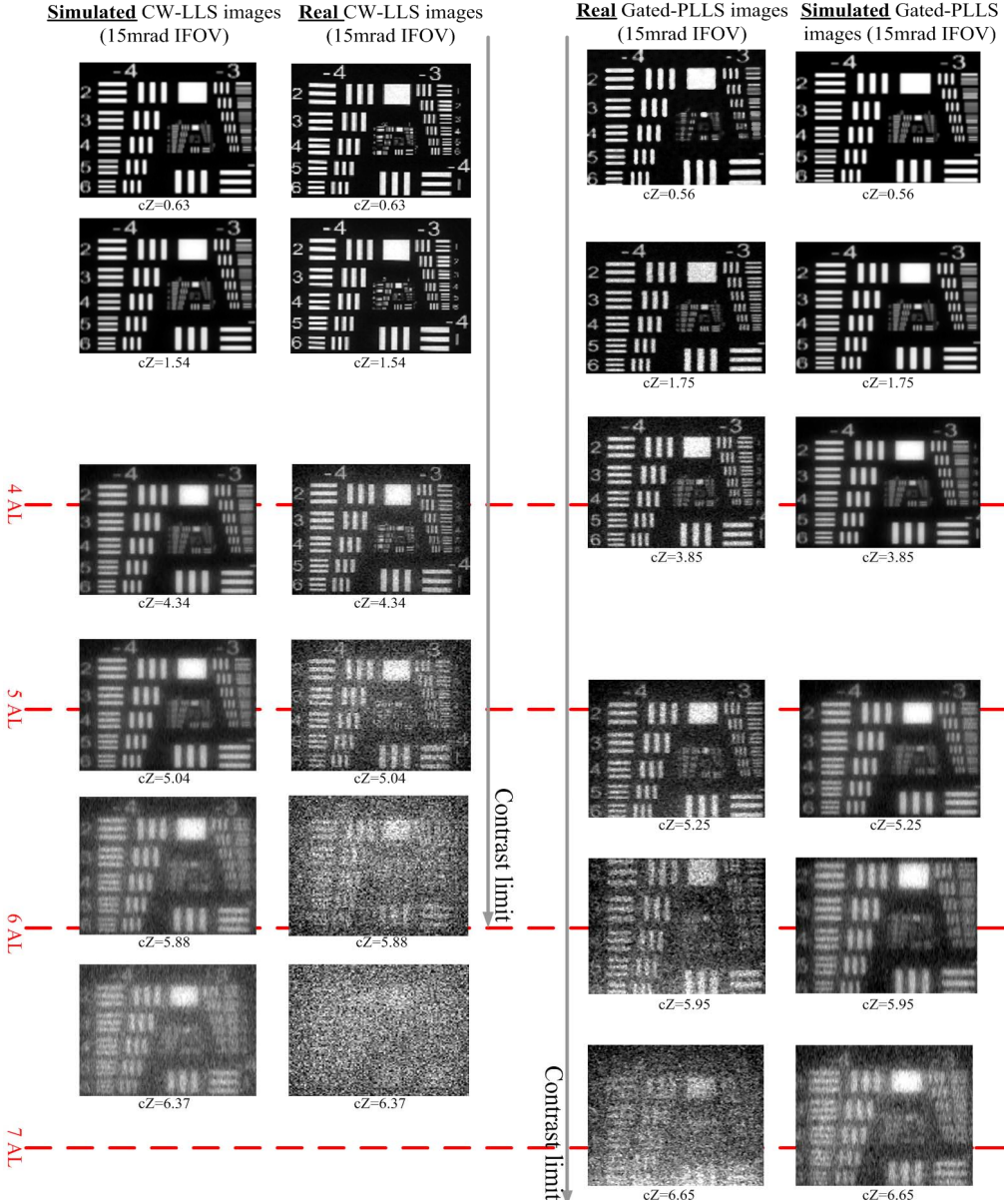


**Figure 2: Gated-PLLS test tank images versus CW-LLS at 7 meters. The outer two columns show the simulated images for each case.  $cZ$  = number of attenuation lengths at 532nm, where  $c$  is the attenuation coefficient and  $Z$  is the distance to the target.**

### 3. Application of Image Quality algorithms to acquired images.

In order to test the T-S autofocus approach using the HBOI test facility we acquired images of artificial targets with ‘ideal’ settings and with intentional image degradation induced by misaligning the receiver. Fig. 3 shows the master image collected, and a target sub-image selected therefrom.

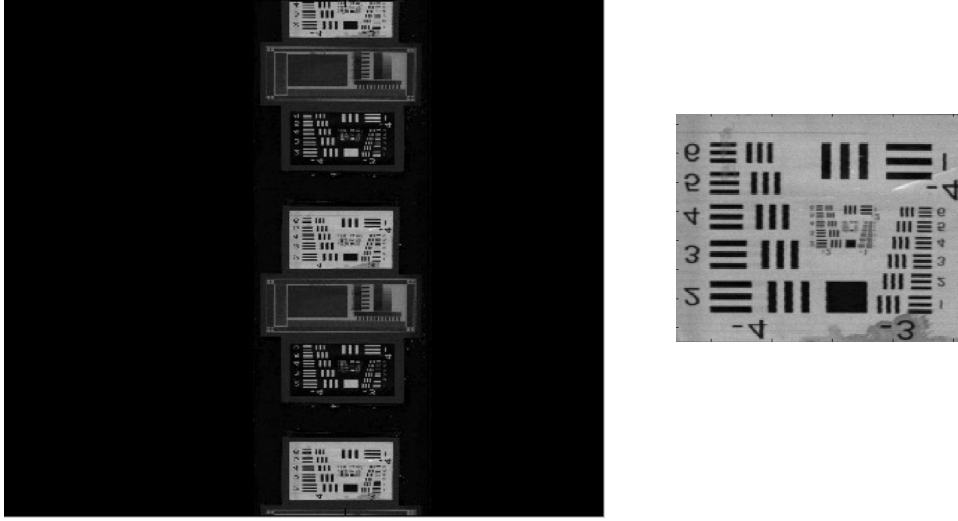


**Figure 3: Master image (left) and selected target image.**

The fitness value computed by the T-S algorithm was nearly identical for the two images of each target selected from the master image, but different from one target to another, showing that the absolute value of the metric is dependent on image content. The fitness values computed from different master images for a given target followed the desired trend – the fitness value decreased as the receiver misalignment increased. The trend matched subjective judgment of relative image quality among the images. An approach of this sort could be applied in the field by varying system parameters on the fly. Because of platform movement the T-S algorithm would be applied to different images, but if the bottom type is relatively consistent at a textural level the images and results could be treated as pseudo-static. The benefit of this approach would be realized in systems in which human operator adjustment is not desired or possible.

For image quality analysis of test tank technical target images, the *contrast* and *contrast signal noise ratio* metric were used. Fig. 4 shows the *contrast* for the CW LLS against the gated-PLLS before and after the images were normalized for laser pulse energy variations. Conventional images acquired using an 18 watt LED spot illuminator with a Nikon D70 camera were used as a baseline comparison. Fig. 5 shows the computed *contrast signal noise ratio* results for the same set of images.

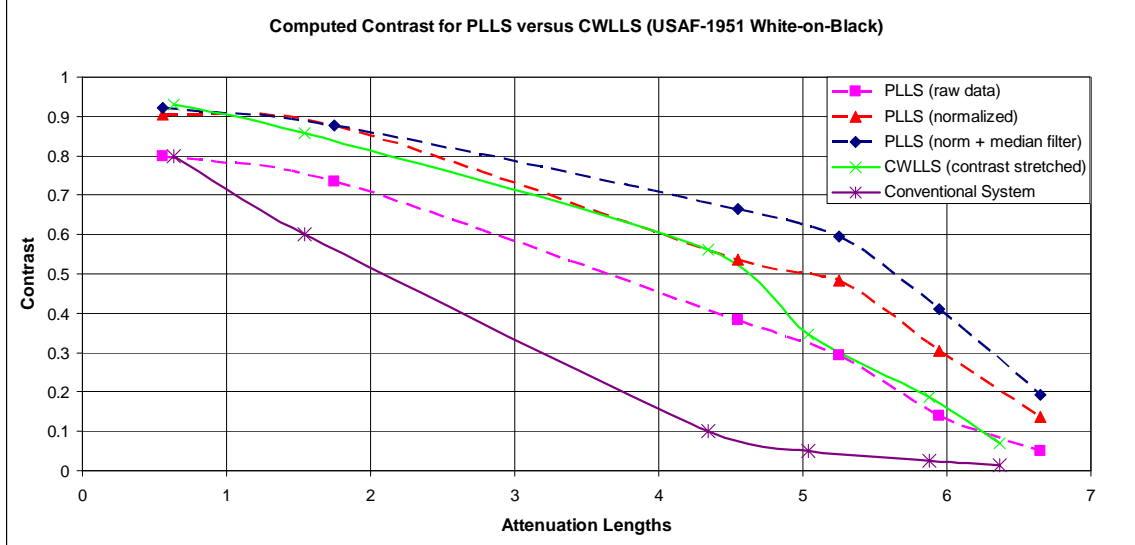


*Figure 4: Contrast versus number of attenuation lengths for gated-PLLS, CW LLS and conventional camera and light.*

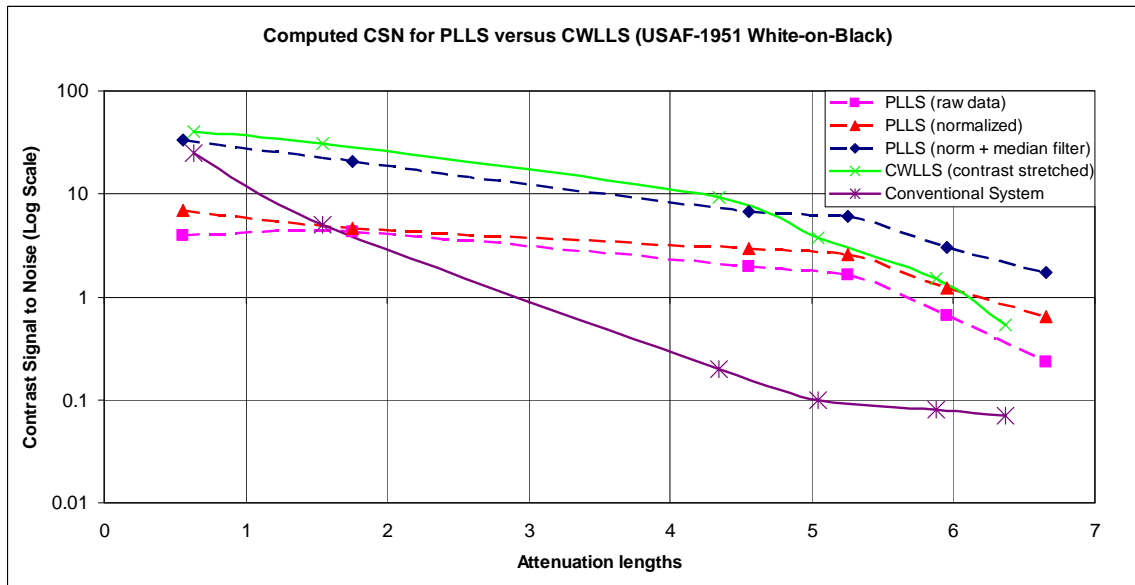


*Figure 5: Contrast Signal Noise Ratio versus number of attenuation lengths for gated-PLLS, CW LLS and conventional camera and light.*

The results show that the gated-PLLS is capable of producing images at more than 1 attenuation length beyond the limit of CW LLS. Increased laser pulse energy and stability, improvements in gated detector performance, together with the use of processing to isolate the acquired pulses from both the gate ringing signal and the tail end of the backscatter signal should further improve performance. The use of shorter pulses and coded pulses are also being examined via advanced simulation work.

#### 4. Advanced simulations and experimental validation for modulated-pulses.

A comparison of the Metron model output versus measured data for the modulated-pulse case is shown on the top plot of each graphset in fig. 6. Aside from system noise in the experimental data, the conformance appears to be satisfactory. IQ demodulation results are also shown for simulated and measured cases in fig. 6.

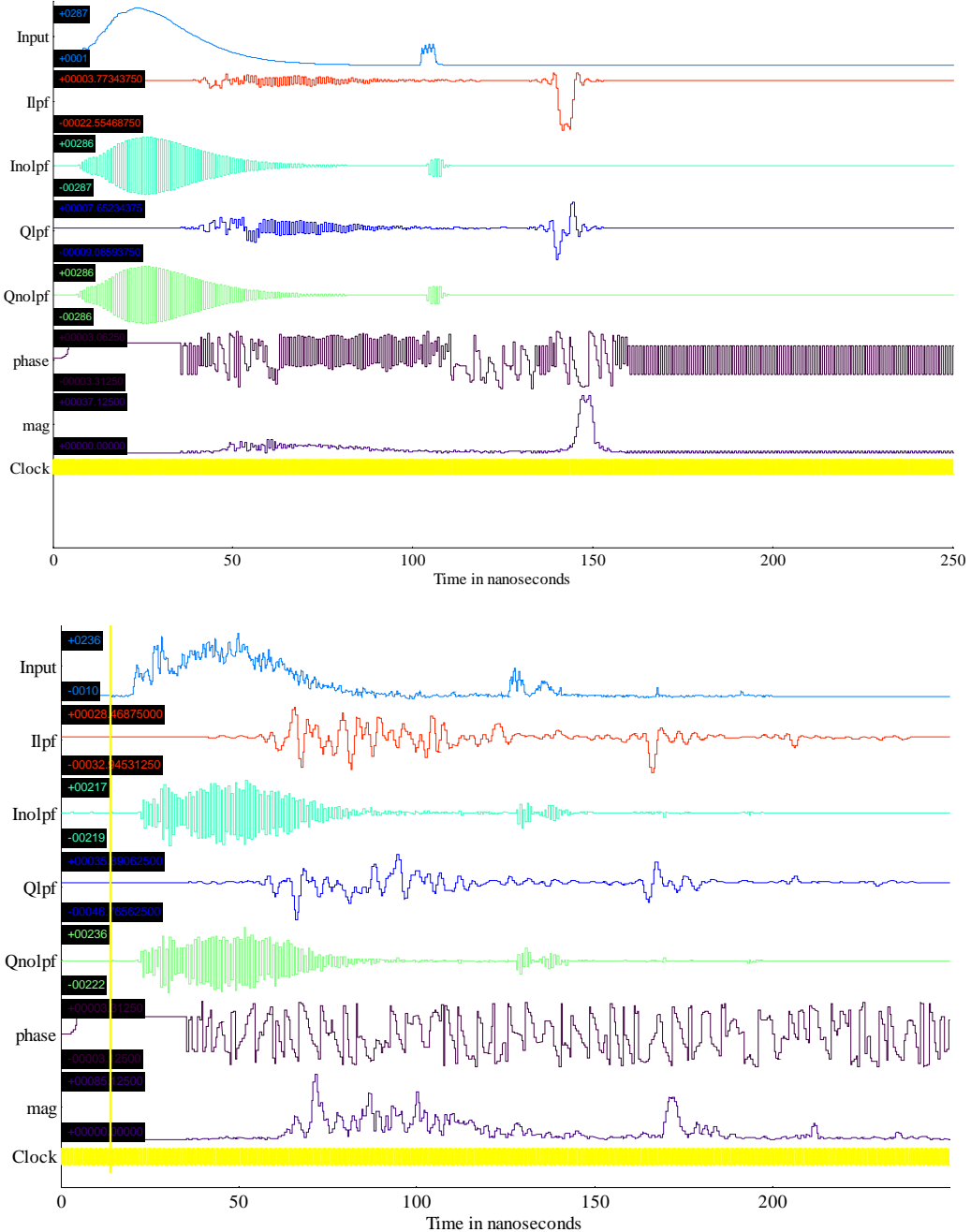


**Figure 6:** Top graphset: Simulation results with Metron time history code and IQ demodulation processing for a 1GHz modulated pulse with 99% target 11.42m distant ( $c=0.58m^{-1}$ ,  $cZ=6.62$ ).  
Bottom graphset: Experimental results from same case.

## **IMPACT/APPLICATIONS**

The gated-PLLS system has shown both analytically and experimentally to be capable of extending the operational range of wide-swath optical imaging systems in turbid water beyond the current state-of-the-art of 5 to 6 attenuation lengths. For example, test-tank results suggest that the limits of operability of the gated-PLLS to be beyond 7 attenuation lengths in turbid coastal conditions. The gated-PLLS does not require a significant source-receiver separation to produce quality images, and hence allows for more compact, simpler optical designs which have the potential to be more immune to changes in operating conditions, and hence more reliable than the current state-of-the-art.

The transitioning of such a system into the Navy's fleet of AUVs would certainly be beneficial in the context of MCM and ISR missions. However the PLLS class of imager not only has benefits in identifying targets of potential military or homeland security interest, but may also be a valuable tool for the AUV survey community, either within the offshore hydrocarbon and telecommunications industries for seabed inspection purposes, or for scientific exploration and environmental monitoring applications.

## **RELATED PROJECTS**

A Navair SBIR phase I has been performed in collaboration with Advanced Technologies Group (Stuart, FL) to develop a high performance gated Lidar-radar receiver for underwater imaging.

## **REFERENCES**

Shih, L., 2007. Autofocus survey: A comparison of algorithms. In Digital Photography III, SPIE Vol. 6502.

## **PUBLICATIONS**

Dalgleish, F. R., Caimi, F. M., Britton, W. B., Andren C. F. and Wan Y. 2008. "Experimental comparison of pulsed-gated and continuous wave LLS underwater imagers." *Ocean Optics XIX. October 6-10 2008, Barga, Italy.*

Dalgleish, F. R., Caimi, F. M., Britton, W. B., Wan, Y., Mazel, C. H., Glynn, J. M., Towle, J. P., Giddings T. and Shirron, J. 2008. "Experimental validation of a laser pulse time history model." *Ocean Optics XIX. October 6-10 2008, Barga, Italy.*

Caimi, F. M., Dalgleish, F. R., Kocak, D. M., and Watson, J. 2008. "Underwater Optics and Imaging: Recent Advances", *Oceans 2008, September 15-18 2008, Quebec City, Canada.*

Kocak, D. M., Dalgleish, F. R., Caimi, F.M., and Schechner, Y.Y. "A Focus on Recent Developments and Trends in Underwater Imaging," *MTS Journal, Spring 2008, 42(1):50-65.*